

1 Inter-annual variations of wet deposition in Beijing during 2014-2017:
2 implications of below-cloud scavenging of inorganic aerosols

3

4 Baozhu Ge^{1,5*}, Danhui Xu¹, Oliver Wild², Xuefeng Yao³, Junhua Wang^{1,4}, Xuechun
5 Chen¹, Qixin Tan^{1,4}, Xiaole Pan¹, Zifa Wang^{1,4,5*}

6 ¹ State Key Laboratory of Atmospheric Boundary Layer Physics and Atmospheric
7 Chemistry (LAPC), Institute of Atmospheric Physics (IAP), Chinese Academy of
8 Sciences (CAS), Beijing 100029, China

9 ² Lancaster Environment Centre, Lancaster University, LA1 4YQ, United Kingdom

10 ³ PLA 96941 Army, Beijing 102206, China

11 ⁴ University of Chinese Academy of Sciences, Beijing, 100049, China

12 ⁵ Center for Excellence in Regional Atmospheric Environment, Institute of Urban
13 Environment, Chinese Academy of Sciences, Xiamen 361021, China

14 *Correspondence to: Baozhu Ge (gebz@mail.iap.ac.cn) and Zifa Wang
15 (zifawang@mail.iap.ac.cn)

16 **Abstract**

17 Wet scavenging is an efficient pathway for the removal of particulate matter (PM) from
18 the atmosphere. High levels of PM have been a major cause of air pollution in Beijing
19 but have decreased sharply under the Air Pollution Prevention and Control Action Plan
20 launched in 2013. In this study, four years of observations of wet deposition have been
21 conducted using a sequential sampling technique to investigate the detailed variation in
22 chemical components through each rainfall event. We find that the major ions, SO_4^{2-} ,
23 Ca^{2+} , NO_3^- and NH_4^+ , show significant decreases over the 2013-2017 period (decreasing
24 by 39%, 35%, 12% and 25%, respectively), revealing the impacts of the Action Plan.
25 An improved method of estimating the below-cloud scavenging proportion based on
26 sequential sampling is developed and implemented to estimate the contribution of
27 below-cloud and in-cloud wet deposition over the four-year period. Overall, the below-
28 cloud scavenging plays a dominant role to the wet deposition of four major ions at the
29 beginning of the Action Plan. The contribution of below-cloud scavenging for Ca^{2+} ,
30 SO_4^{2-} and NH_4^+ decreases from above 50% in 2014 to below 40% in 2017. This suggests
31 that the Action Plan has mitigated PM pollution in the surface layer and hence decreased
32 scavenging due to the washout process. In contrast, we find little change in the annual
33 volume weighted average concentration for NO_3^- where the contribution from below-
34 cloud scavenging remains at ~44% over the period 2015-2017. While highlighting the
35 importance of different wet scavenging processes, this paper presents a unique new
36 perspective on the effects of the Action Plan and clearly identifies oxidized nitrogen
37 species as a major target for future air pollution controls.

38 **Key words:** wet scavenging, below-cloud, in-cloud, deposition, $\text{PM}_{2.5}$

39

40 **1 Introduction**

41 Atmospheric wet deposition is a key removal pathway for air pollutants and is governed
42 by two main processes: in-cloud and below-cloud scavenging (Goncalves et al., 2002;
43 Andronache, 2003, 2004a; Henzing et al., 2006; Sportisse, 2007; Feng, 2009; Wang et
44 al., 2010; Zhang et al., 2013). The below-cloud scavenging process depends both on
45 the characteristics of the rain (snow), including the raindrop size distribution and
46 rainfall rate, and on the chemical nature of the particles and their concentration in the
47 atmosphere (Chate et al., 2003). Previously, below-cloud scavenging was thought to be
48 less important than in-cloud processes and was simplified or even ignored in many
49 global and regional chemical transport models (CTMs) (Barth et al., 2000; Tang et al.,
50 2005; ENVIRON.Inc, 2005; Textor et al., 2006; Bae et al., 2010). However, more recent
51 extensive research on wet scavenging has found that precipitation, even light rain, can
52 remove 50-80% of the number or mass concentration of below-cloud aerosols, and this
53 is supported by both field measurements and semi-empirical parameterizations of
54 below-cloud scavenging in models (Andronache, 2004b; Zhang et al., 2004; Wang et al.,
55 2014). Xu et al. (2017; 2019) studied the below-cloud scavenging mechanism based on
56 the simultaneous measurement of aerosol components in rainfall and in the air in
57 Beijing. They found that below-cloud scavenging coefficients for PM_{2.5} widely used in
58 CTMs ($\sim 10^{-5}$ - 10^{-6}) were 1-2 orders of magnitude lower than estimates from
59 observations (at the range of 10^{-4} - 10^{-5} for SO₄²⁻, NO₃⁻ and NH₄⁺, respectively). This
60 implies that the simulated below-cloud scavenging of aerosols might be significantly
61 underestimated. This could be one reason for the underestimation of SO₄²⁻ and NO₃⁻
62 wet deposition in regional models of Asia reported in phase II and III of the Model
63 Inter-Comparison Study for Asia (MICS-Asia) (Wang et al., 2008; Itahashi et al., 2020;
64 Ge et al., 2020) and in global model assessments by the Task Force on Hemispheric
65 Transport of Atmospheric Pollutants (TF-HTAP) (Vet et al., 2014), in addition to the
66 other sources of model uncertainties (Chen et al., 2019; Tan et al., 2020; Kong et al.,
67 2020), such as emissions, chemical transformation and changes in other ambient
68 compounds of sulfur and nitrogen. Bae et al. (2012) added a new below-cloud
69 scavenging parameterization scheme in the CMAQ model and improved the simulation

70 of aerosol wet deposition fluxes in East Asia by as much as a factor of two compared
71 with observations. The below-cloud scavenging process is critical not only for wet
72 deposition but also for the concentration of aerosols in the air and it should be
73 represented appropriately in CTM simulations.

74 It is important to recognize the contribution of below-cloud scavenging to total wet
75 deposition. However, many studies have found that it is difficult to separate the two wet
76 scavenging processes based on measurement methods alone (Huang et al., 1995; Wang
77 and Wang, 1996; Goncalves et al., 2002; Bertrand et al., 2008; Xu et al., 2017). A
78 commonly used approach to separating below-cloud scavenging from total wet
79 deposition is through sequential sampling (Aikawa et al., 2014; Ge et al., 2016; Aikawa
80 and Hiraki, 2009; Wang et al., 2009; Quyang et al., 2015; Xu et al., 2017). In this way,
81 precipitation composition during different stages of a rainfall event can be investigated
82 separately in the lab after sampling. The chemical components in later increments of
83 rainfall are thought to be less influenced by the below-cloud scavenging process than
84 by the in-cloud scavenging process (Aikawa et al., 2014; 2009). Xu et al. (2017) applied
85 this approach to summer rainfall in Beijing in 2014 and found that more than 50% of
86 deposited sulfate, nitrate and ammonium ions were from below-cloud scavenging. In
87 this study, an innovated method based on exponential curve to chemical ions in rainfall
88 by sequential sampling is developed and implemented to estimate the ratio of below-
89 cloud to in-cloud wet deposition in Beijing over the four-year period between 2014 and
90 2017. Together with PM_{2.5} concentration measurements, the below-cloud scavenging
91 effects of the decreasing air pollutants at near-surface due to the Air Pollution
92 Prevention and Control Action Plan (Action Plan) launched in 2013 (State Council of
93 the People's Republic of China, 2019) is also investigated to explore the implications
94 of the Action Plan to the precipitation chemistry.

95 **2 Data and methods**

96 **2.1 Measurement site and sampling methodology**

97 The measurement site is located on the roof of a two-floor building at the Institute of
98 Atmospheric Physics tower site (IAP-tower, 39° 58' 28" N, 116° 22' 1" E) in northern
99 Beijing. It is a typical urban site between the 3rd and 4th ring roads and lying close to

100 the Badaling expressway (Xu et al., 2017;2019;Sun et al., 2015). Four years of Inter-
101 annual observations of each rainfall event were conducted at this site. Sequential
102 sampling of each rainfall event is employed to catch the evolution of precipitation
103 composition during each event. To investigate the detailed variation in the concentration
104 of different chemical components in precipitation, especially the sharp changes
105 occurring during the onset of rainfall, high resolution sampling of rainfall at 1 mm
106 sequential increments was performed using an automatic wet-dry sampler. The
107 rainwater collector uses a circular polyethylene board with a 30 cm diameter and
108 collects up to eight fractions. About 70 ml of rainwater is collected for each of the first
109 seven fractions and the rest of the rainfall is collected in the eighth fraction. For example,
110 if there is 12 mm rainfall volume in a precipitation event, 1 mm sequential rainfall is
111 collected in each of the first 7 fractions with the rest of 5 mm in the eighth fraction.
112 Rainfall events where eight fractions are collected and identified as full events, and
113 those with fewer than eight fractions are characterized as incomplete events. Manual
114 sampling methods were used to collect more than eight fractions during heavy rainfall,
115 and these are characterized as extended events. During 2014-2017, a total of 104
116 precipitation events, which is almost 690 precipitation samples, were collected. Of the
117 total number of precipitation events, 33 events (32%) were discarded from the
118 sequential sampling analysis due to low rainfall amounts (<8 mm), which cannot satisfy
119 the rules of full events. Altogether, 69 full events including 6 extended events were
120 recorded over the 2014-2017 period in Beijing, as 15, 16, 20 and 18 events at each year,
121 respectively. The rainfall volume of the eighth fraction of these 69 full events varied
122 from 1 mm to 55.9 mm.

123 After collection, all samples are refrigerated at 0-4 °C and analyzed at the Key
124 Laboratory for Atmospheric Chemistry, Chinese Academy of Meteorological Sciences
125 (CAMS) within one month, following the procedure used for the Acid Rain Monitoring
126 Network run by the China Meteorological Administration (CMA-ARMN) (Tang et al.,
127 2007;2010). Nine ions that include four anions (SO_2^+ , NO_3^- , Cl^- and F^-) and five cations
128 (NH_4^+ , Na^+ , K^+ , Ca^{2+} and Mg^{2+}) are detected using ion chromatography (IC, Dionex
129 600, USA). Their relative standard deviations in reproducibility tests are less than 5%.

130 Quality assurance is carried out using routine standard procedure of blind sample inter-
131 comparison organized by CMA (Tang et al., 2010). Quality control is conducted by
132 assessment of the anion-cation balance and by comparison of the calculated and
133 measured conductivity. A more detailed description of the procedure can be found in
134 Ge et al. (2016) and Xu et al. (2017).

135 **2.2 Aerosol measurements**

136 Aerosol mass concentration is recorded in routine measurements for the observation
137 network of the China National Environmental Monitoring Center (CNEMC). PM_{2.5}
138 concentrations are used from the Olympic Park station, a monitoring station located 3
139 km to the northeast of the IAP-tower sampling site. In addition, an Ambient Ion
140 Monitor-Ion Chromatograph (AIM-IC) developed by URG Corp., Chapel Hill, NC and
141 Dionex Inc., Sunnyvale, CA, is used to measure PM_{2.5} composition at the sampling site
142 between 2014 and 2017. This instrument includes a sample collection unit (URG 9000-
143 D) for collection of water-soluble gases and particles in aqueous solution and a sample
144 analysis unit (two ion chromatographs, Dionex ICS-2000 and ICS-5000) for analysis
145 of both anions and cations. The limit of detection of AIM-IC is 0.08 mg/m³ for NH₄⁺
146 and 0.1 mg/m³ for the other ions. Aerosol mass concentrations and composition are both
147 measured at 1 h time resolution. Detailed descriptions of the AIM-IC instrumentation
148 can be found in Malaguti et al. (2015) and Markovic et al. (2012). The average
149 concentration of aerosols in the 6 h before each rainfall event is calculated to reflect the
150 air pollution conditions before the event. For comparisons, the yearly average
151 concentration of aerosols has been calculated to represent the normal conditions.

152 **2.3 Estimation of below cloud scavenging**

153 Previous studies have shown that the concentration of chemical ions in precipitation
154 decreases through the progression of a rainfall event and eventually stabilizes at low
155 levels (Aikawa and Hiraki, 2009;2014;Ge et al., 2016;Xu et al., 2017). The in-cloud
156 and below-cloud scavenging contributions to total wet deposition are estimated based
157 on the assumption that the concentrations in later increments can be attributed to
158 scavenging by rainout only. According to (Seinfeld and Pandis, 2006), species can be
159 incorporated into cloud and raindrops inside the raining cloud and this process

160 determine the initial concentration of raindrops before they start falling below the cloud
161 base. In this stage, despite of the efficient process of the nucleation scavenging in cloud,
162 the total mass of aerosol in cloud is almost stable due to the slow process of interstitial
163 aerosol collection by cloud droplets which is the determination process to aerosol mass.
164 That is to say, the initial concentration of raindrops in cloud is well mixed and can be
165 considered as a stable statue during the whole rainfall event. That is why many
166 observations in different regions (Aikawa *et al.*, 2009; 2014; Wang *et al.*, 2009; Quyang
167 *et al.*, 2015; Xu *et al.*, 2017) reported that the chemical components in a rainfall event
168 show a decayed variation with the increase of precipitation amount and eventually tends
169 to a stable and low concentration level. The assumption in this study as well as the
170 previous studies is based on this fact. It does not mean the below-cloud and in-cloud
171 scavenging occur in sequence. But, instead, the two processes have been mixed in all
172 stage of the rainfall event with the below-cloud scavenging contributed more in
173 beginning fraction and the in-cloud scavenging contributed more in the later fraction
174 due to the depletion of the air pollutants below cloud by washout.

175 This assumption relies on the efficient scavenging of air pollutants below cloud
176 through the evolution of precipitation. However, the concentration of chemical ions in
177 precipitation may also be affected by many other factors in addition to below-cloud air
178 pollutant concentrations and in-cloud scavenging processes. For example, the
179 precipitation intensity may affect the scavenging efficiency of air pollutants below
180 cloud and hence influence wet deposition (Andronache, 2004b; Wang *et al.*, 2014; Xu *et al.*
181 *et al.*, 2017; 2019). Yuan *et al.* (2014) reported that in central North China high intensity
182 rainfall events of short duration (lasting less than 6 h) are dominant rather than long-
183 duration rainfall that is more common in the Yangtze River Valley. Therefore, the time
184 window for the definition of in cloud stage is very important for estimating the below
185 cloud and in cloud contributions. Previous studies have estimated the concentration of
186 chemical ions scavenged in-cloud based on the judgment that 5 mm of accumulated
187 precipitation is sufficient to identify the contribution of the in-cloud scavenging process
188 (Wang *et al.*, 2009; Aikawa and Hiraki, 2009; Xu *et al.*, 2017). Based on this approach,
189 the concentration of NO_3^- and SO_4^{2-} in cloud in Japan was found to be 0.70 and 1.30

190 mg/L, respectively (Aikawa and Hiraki, 2009). In Beijing, high concentration of NH_4^+ ,
191 SO_4^{2-} and NO_3^- during 2007 were found at 2.1~5.5, 3.1~14.9, 1.5~5.9 mg/L,
192 respectively (Wang et al., 2009; Xu et al., 2017).

193 In this study, a new method based on fitting a curve to the chemical ion
194 concentrations with successive rainfall increments has been developed to estimate the
195 contribution of the in-cloud process. As shown in Figure 1, an exponential curve is
196 fitted to the median, 25th and 75th percentiles of the chemical ion concentrations in each
197 fraction through the rainfall increments. Noted that, the fitted exponential curve is
198 applied to the combination of all 69 full events to estimate the yearly median
199 concentration of chemical ions in-cloud and to compare with the results from previously
200 reported method (i.e., median concentration after 5 mm increments). Besides, the
201 exponential approach to each unique event was also employed. Ideally, the
202 concentration of chemical ions stabilize at higher rainfall increments and this represents
203 the concentration in cloud. However, the decrease during each rainfall event is distinctly
204 different, and this regression method is not fully applicable to all rainfall events in
205 practice. Therefore, the exponential regression method is used to estimate the in-cloud
206 concentration under most circumstances, but where the decreasing trend with the
207 increment of rainfall is not significant, the average value of rainfall increments 6-8 of
208 the event is used. The below cloud contributions to wet deposition of each species are
209 then calculated using the following equations (1-2):

$$210 \quad \text{Wetdep}_{\text{below-cloud}} = \sum_{i=1}^n (C_i - \bar{C}) \times P_i \quad (1)$$

$$211 \quad \text{Contribution}_{\text{below-cloud}} = \frac{\text{Wetdep}_{\text{below-cloud}}}{\sum_{i=1}^n C_i \times P_i} \quad (2)$$

212 Where, C_i , and \bar{C} represent the concentration of each chemical ion in fraction i and in
213 cloud and P_i represents the volume of rainfall, while n represent the total fractions in
214 a rainfall event (equally to 8 in this study).

215 **3 Results and Discussion**

216 **3.1 Inter-annual variations in chemical components**

217 The Action Plan is launched in 2013 called “Ten rules” to improve the air quality in
218 China. It includes comprehensive control of industrial emission, non-point emission,

219 fugitive dust, vehicles, etc. It is also aimed to adjust and optimize the industrial
220 structure and promote economic transformation and upgrading, such as increase the
221 supply of clean energy. These actions are ensured to work by both of legislation and
222 market mechanism. According to the *Beijing Environmental Statement* published by the
223 Beijing Municipal Environmental Protection Bureau from 2013 to 2017, many
224 measures have been implemented to meet the Action Plan, including replacement
225 residential coal with electricity and natural gas, upgrading the emission standards of
226 gasoline, diesel vehicles and power plants, closing the high-emission enterprises.
227 Significant declines in atmospheric PM_{2.5} concentration have been observed nationwide
228 between 2013 and 2017 during the Action Plan (Zhang et al., 2019). However, few
229 studies have investigated the benefits of the Action Plan for wet deposition. A
230 significant increase in NO₃⁻ in precipitation of 7.6% was observed at a regional
231 background station in North China between 2003 and 2014 (Pu et al., 2017). A decrease
232 in the ratio of SO₄²⁻/NO₃⁻ mostly due to the decreasing of SO₄²⁻ and increasing of NO₃⁻
233 suggests the transformation of sulfuric acid type to a mixed type of sulfuric and nitric
234 acid in North China. However, the updated record especially after the Action Plan is
235 important to assess the mitigation of the air pollutants not only in the atmosphere but
236 also in rainfall. A nationwide investigation of the wet deposition of inorganic ions in
237 320 cities across China was recently made based on observations between 2011 and
238 2016 from the National Acid Deposition Monitoring Network (NADMN), which was
239 established by the China Meteorological Administration (Li et al., 2019). Briefly, both
240 SO₄²⁻ and NO₃⁻ across China experienced significant changes before and after 2014,
241 with increases from 2011 to 2014 and then decreases from 2014 to 2016.

242 In order to quantify the influence of the Action Plan on wet deposition in Beijing,
243 four years of observations of each rainfall event are considered in this study. Figure 2
244 shows the volume weighted average (VWA) of inter-annual mean concentrations of
245 SO₄²⁻, NO₃⁻, NH₄⁺ and Ca²⁺ observed in Beijing during 2014 to 2017 along with those
246 reported before 2010 from previous studies (Yang et al., 2012; Pan et al., 2012, 2013)
247 (more detail is provided in Table S1 in supplementary materials). A continuous
248 decrease in VWA concentrations between 1995 and 2017 is found for SO₄²⁻, with

249 decreases of 3.1% yr⁻¹ in the earlier stage (1995-2010) and decreases of 9.8% yr⁻¹ in the
250 later stage (2014-2017). This is consistent with the annual changes in its emission and
251 concentration as shown in Figure 3, in which the emission and the concentration data
252 are collected from the yearly book of “*Environmental Bulletin in Beijing*” from 1994 to
253 2017. It is clearly shown the concentration of SO₂ experienced a sustainably decreasing
254 trend due to significant reduction of its emission from 1996 to 2017, with the decreases
255 rate is 4.5% yr⁻¹ and 13.9% yr⁻¹ in emission and 2.8% yr⁻¹ and 14.0% yr⁻¹ in
256 concentration during earlier stage and the later stage (the Action Plan period),
257 respectively. The significant declines in VWM concentration of Ca²⁺ is found in
258 precipitation with the decreases rate as 36.1% yr⁻¹ in 1995-2010 and 8.8% yr⁻¹ in 2014-
259 2017. The emission and the concentration data of Ca²⁺ are absent in this study. Instead,
260 the different of PM₁₀ and PM_{2.5} (PM₁₀-PM_{2.5}) concentration during 2013-2017 have
261 been calculated to represent the coarse particles, which mainly contains the Ca²⁺ as well.
262 The results show that the concentration decreased from 31.2 μg/m³ in 2013-2014 to
263 24.0 μg/m³ over 2015-2017. This indicates the improvement of coarse particles even
264 which is derived from crustal emissions have been made through the Action Plan. As
265 that is mentioned above, the Action Plan including emission reduction not only from
266 energy consumption of industry but also the fugitive dust in cities, which should result
267 the decline in Ca²⁺. For NO₃⁻ and NH₄⁺, increases are found during the earlier stage
268 (~60%) and decreases in the later stage (12% for NO₃⁻ and 25% for NH₄⁺). As to NO_x
269 emission, the data in recent years have been collected. Although the clearly reduction
270 is found in the annual changes of emission from 2010, the ambient concentration of
271 NO₂ do not show a significant decreasing trend (~3.6% yr⁻¹) compared with SO₂ (14%
272 yr⁻¹). However, before the Action Plan, the decreasing ratio in concentration is only 1.8%
273 yr⁻¹, which is slower than the Action Plan period. Despite the increases of VWA NO₃⁻
274 in precipitation during the earlier stage, the small decreases in later stage would also be
275 attributed to the Action Plan.

276 For a better understanding of the impacts of acidification on ecosystems, wet
277 deposition fluxes of the four major ions in precipitation are also plotted in Figure 2.
278 Similar variations are found as that presented in VWA of the four major ions.

279 Observations on S and N wet deposition (Pan et al., 2012; 2013) during 2007-2010
280 show the value of 21.5 kg S ha⁻¹ yr⁻¹ and 27.9 kg N ha⁻¹ yr⁻¹ (19.7 and 8.2 kg N ha⁻¹ yr⁻¹
281 ¹ through NO₃⁻ and NH₄⁺) in Beijing, respectively. Compared with those results,
282 significant decreases (11.4 kg S ha⁻¹ yr⁻¹ and 23.6 kg N ha⁻¹ yr⁻¹) were observed in the
283 four-years measurements during 2014-2017 in this study. All four components in the
284 later stage show significant decreases, suggesting that the Action Plan, which was
285 implemented over this period, has a substantial impact. While Ca²⁺ and SO₄²⁻ played a
286 prominent role in precipitation during the earlier stage before 2010, NH₄⁺ and NO₃⁻
287 became the primary components in the later stage after 2010. It should be noted that
288 NH₄⁺ has a double role in environment pollution because it mitigates acid rain through
289 neutralization, but also acidifies the soil by nitrification. Hence, while sulfur in
290 precipitation has been further reduced under the Action Plan, additional attention is
291 needed for nitrogen to prevent deterioration of the environment by acid rain resulting
292 from nitrate and ammonium.

293 **3.2 Relationship in concentrations in precipitation and the atmosphere**

294 Wet deposition of a substance involves its removal from the associated air mass. The
295 scavenging ratio H can be estimated by comparing the monthly average concentration
296 in precipitation with that in the air (Okita et al., 1996; Kasper-Giebl et al., 1999; Hicks,
297 2005; Yamagata et al., 2009). Xu et al. (Xu et al., 2017) first calculated the rainfall event
298 H based on the hourly concentration of aerosol components measured with an Aerodyne
299 Aerosol Chemical Speciation Monitor (ACSM) and AIM-IC in 2014. In this study four
300 years of observation of aerosol components have been undertaken by AIM-IC.
301 Measurements made in the 6 hours before each rainfall event are averaged to represent
302 the precondition of wet deposition precursors in the atmosphere. Figure 4 shows the
303 relationship between the major chemical ions in precipitation and in the air. The VWA
304 concentration of SO₄²⁻, NO₃⁻ and NH₄⁺ (hereafter SNA) as well as Ca²⁺ in each rainfall
305 event has been calculated and compared with that in the first 1 mm rainfall fraction,
306 F1#. As shown in Figure 4, positive correlations are found between the concentrations
307 of ions in precipitation and in air, with Pearson correlation coefficients (R) generally
308 higher than 0.7 (p<0.01). The concentration in the first fraction should represent a high

309 proportion of below-cloud scavenging due to the washout of air pollutants below clouds
310 by the first rainfall, while the VWA represents a greater contribution from in-cloud
311 removal (Aikawa and Hiraki, 2009; Wang et al., 2009; Xu et al., 2017). Thus, it is
312 reasonable that the correlations are stronger for the first fraction than for the VWA, see
313 Table 1. This indicates that the concentration of chemical ions in precipitation at the
314 start of rainfall is more greatly influenced by the air pollutants below the cloud. As
315 rainfall continues and below-cloud concentrations are reduced, there is an increased
316 contribution from in-cloud scavenging, which is less influenced by aerosols in the
317 surface layer. This is confirmed by the substantial difference in the two R coefficients
318 for the cation ion Ca^{2+} (0.85 for the first fraction, 0.47 for the VWA), which often exists
319 in coarse particles below cloud. For the fine particle SO_4^{2-} which is present both in and
320 below clouds (Xu et al., 2017), the difference in the two R coefficients is small. The R
321 coefficients for NO_3^- and NH_4^+ show less difference than Ca^{2+} , but larger difference
322 than SO_4^{2-} . This may relate to their complicate sources from the ambient precursors.
323 For example, the NO_3^- in precipitation is both from the fine and coarse particles (i.e.,
324 particulate NO_3^-) as well as the gaseous HNO_3 , while the NH_4^+ in precipitation is mainly
325 from the fine particles in addition to NH_3 .

326 The slope of the linear fits in Figure 4 can be used to calculate the scavenging ratio
327 W , which is the ratio of the ions concentration in precipitation (mg/L) and in air ($\mu\text{g}/\text{m}^3$).
328 The W ratio is 0.25×10^6 , 0.16×10^6 and 0.15×10^6 for SNA, SO_4^{2-} , NO_3^- and NH_4^+
329 respectively. This is similar to that reported for rainfall events in 2014 in Beijing
330 (0.26×10^6 , 0.35×10^6 and 0.14×10^6 for SNA) by Xu et al. (2017) and consistent with
331 those estimated in the eastern United States ($0.11\text{-}0.38 \times 10^6$, $0.38\text{-}0.97 \times 10^6$ and 0.2-
332 0.75×10^6 for SNA) (Hicks, 2005). Compared with SO_4^{2-} and NH_4^+ , the scavenging ratio
333 for NO_3^- shows larger differences between this study and previous studies,
334 corresponding to larger uncertainties to the R between the concentrations of ions in
335 precipitation and in air for VWA in Figure 4a (lower significance $p < 0.05$). It should be
336 noted that the W calculated in this study is based on the fine particles in air, which
337 may not represent the accurate reflection of the wet scavenging efficiency of SNA.
338 These uncertainties have been evaluated. For S, gas SO_2 was considered to testified its

339 role to the relationships. Figure S1 shows the relationships between the concentration
340 of SO_4^{2-} in precipitation and in air (SO_4^{2-} in precipitation vs SO_4^{2-} , and SO_4^{2-} in
341 precipitation vs $\text{SO}_2+\text{SO}_4^{2-}$). The correlation coefficients R increased if the role of gas
342 SO_2 was considered (R of SO_4^{2-} in precipitation vs SO_4^{2-} is 0.7, and R of SO_4^{2-} in
343 precipitation vs $\text{SO}_2+\text{SO}_4^{2-}$ is 0.75). However, the scavenging ratio W was not
344 changed, with the difference lower than 1%. For N, the contribution of gaseous HNO_3
345 to total inorganic nitrate is less than 2% in NCP according to Zhai et al. (2021), which
346 can be ignored in this study. According to more than one-year measurements in Beijing
347 (Tian et al., 2016), SO_4^{2-} , NO_3^- and NH_4^+ in coarse particles account for 18%, 27% and
348 10%, respectively. The lower coefficient R in NO_3^- than SO_4^{2-} and NH_4^+ in Figure 4 is
349 attributed to the absent of considering NO_3^- in coarse particles. Besides, due to high
350 concentration of NH_3 at ground surface over NCP (Pan et al., 2018), the NH_4^+ in
351 precipitation from gaseous NH_3 cannot be ignored (Kasper-Giebl et al., 1999). The ratio
352 of $\text{NH}_4^+/(2\text{SO}_4^{2-}+\text{NO}_3^-)$ in precipitation and in $\text{PM}_{2.5}$ was calculated. The lower ratio in
353 precipitation than that in $\text{PM}_{2.5}$ was found, with 0.95-1.01 in precipitation and 1.35 in
354 air. This implicated the impacts of rich gas NH_3 at ground surface going into the
355 precipitation by reacting with gaseous HNO_3 and forming as NH_4NO_3 after $(\text{NH}_4)_2\text{SO}_4$.
356 Thus, the contribution of coarse particles and gases to the relationships of S and N
357 compounds in precipitation and the atmosphere is not as important as the fine particles,
358 except NO_3^- in coarse particles and the gaseous NH_3 , which should be considered in the
359 future.

360 Wet deposition can affect much of the atmospheric column through in-cloud and
361 below-cloud scavenging processes. The vertical column density (VCD) of SO_2 and NO_2
362 from satellite during 2000s to 2017 is used here to compare with the inter-annual
363 variations in wet deposition in Beijing (Figure S2). Consistent variation of the VCD
364 and the yearly VWA concentration in precipitation is found in S and N. A continuous
365 decrease is found in VCD SO_2 from 2005 to 2017, matching the trend in SO_4^{2-}
366 deposition, while for VCD NO_2 shows an increase from 2001 to 2011, a decrease after
367 2011 and little change over the period 2014-2017. This implies that the Action Plan not
368 only benefits air pollutants in the surface layer but also those in the total column. Due

369 to faster decreases in emissions of S than N (Zheng et al., 2018), the ratio of S/N in both
370 precipitation ($\text{SO}_4^{2-}/\text{NO}_3^-$, $\mu\text{eq/L}$) and air ($\text{SO}_4^{2-}/\text{NO}_3^-$, $\mu\text{g/m}^3$) are found to decrease,
371 with the change in ratio in precipitation at 17.5% yr^{-1} , 11% yr^{-1} and 20.0 % yr^{-1} during
372 1995-2010, 2014-2017 and 1995-2017, and in air at 12% yr^{-1} during 2014-2017,
373 respectively, see Figure S3. This is also consistent with the trend reported in whole
374 China during 2000-2015 by Itahashi et al. (2018). The ratio of S/N in precipitation is a
375 useful index to investigate the relative contributions of these acidifying species. In
376 addition, the ratio of $\text{NH}_4^+/\text{NO}_3^-$ is investigated here and a clear decrease is found during
377 2014-2017 both in precipitation and in air. This indicates that NH_4^+ is decreasing faster
378 than NO_3^- . This evidence clearly confirms that nitrate should be the major target for air
379 pollution controls in the next Action Plan.

380 **3.3 Proportion of below cloud scavenging**

381 As described in section 2.3, the in-cloud ion concentration (\bar{C} , in Eq 1) can be derived
382 from the exponential fit of the observed rainwater concentrations. Table 2 lists the
383 asymptote value and the exponential fitting equation of the evolution of each ion
384 concentration in precipitation with the increment of rainfall. As shown, the asymptote
385 value (here after, exponential approach) based on the median data for SO_4^{2-} , NO_3^- and
386 NH_4^+ was 3.18 mg/L, 2.32 mg/L and 1.39 mg/L, respectively. The SO_4^{2-} and NO_3^- are
387 within the range of reported in cloud concentrations for Beijing (3.33 mg/L and 2.75
388 mg/L for SO_4^{2-} and NO_3^- in Xu et al., 2017), while the NH_4^+ in this study is lower than
389 previous studies (2.51 mg/L in Xu et al., 2017 and 2.1-4.5 mg/L in Wang et al., 2009).
390 In-cloud concentrations for other ions, i.e., Ca^{2+} , F^- , Cl^- , Na^+ , K^+ and Mg^{2+} , are 0.67
391 mg/L, 0.04 mg/L, 0.27 mg/L, 0.1 mg/L, 0.06 mg/L and 0.08 mg/L, respectively. For
392 comparison, the average concentration in fractions 6 to 8 (F6#~F8#) in each rainfall
393 event (here after, average approach) is used to estimate the in-cloud concentration for
394 events where successive rainwater concentrations do not show an obvious decrease or
395 where other factors such as precipitation intensity are important, see Table 2. Similar
396 results are found for most ions with the exponential and average approach except for
397 NH_4^+ , F^- , K^+ and Mg^{2+} , where the maximum difference is less than 20% (Table 2). Thus,
398 the replacement of in-cloud concentration by the average value is acceptable for SO_4^{2-} ,

399 NO_3^- , Ca^{2+} , Cl^- and Na^+ but much uncertainty for the other ions. It is worth noting that
400 for all ions the average approach gives higher estimates of in-cloud concentrations, and
401 this can be recognized as an upper limit for in-cloud concentrations. It is also important
402 to note that the increased concentrations of ions in the latter fractions were observed in
403 few events in this study. This may due to the unique meteorological conditions and air
404 pollutants movement during each precipitation. Despite the longer precipitation
405 fractions in this study were collected, more longer fraction measurements and more
406 detailed analysis on the uncertainties are needed in the future. The influences of
407 meteorological conditions (i.e., rainfall type and intensity) are discussed in section 4.

408 The model study in Japan showed consistent fractions of in-cloud and below-cloud
409 scavenging to total wet deposition between simulated and observed values, except one
410 site, where is the region of high emission flux of SO_2 . In this region, the simulated
411 below-cloud scavenging contribution was apparently greater than the observed results.
412 Specifically, the model shows the SO_2 and HNO_3 gases dominantly contributed to the
413 below-cloud scavenging of SO_4^{2-} and NO_3^- in the regions of high emission flux of SO_2 ,
414 in while the aerosol removal was dominated by the in-cloud scavenging process. In
415 their model set up, all of below-cloud gas SO_2 was assumed to be dissolved into
416 raindrop and be fully oxidized to SO_4^{2-} . However, as suggested by Seinfeld and Pandis
417 (2006), the aqueous equilibrium between ambient gas and precipitation cannot be
418 assumed due to the relatively short residence times of falling precipitation. Thus, the
419 assumptions used in Kajino et al. (2015) might overestimate the contribution of gas SO_2
420 to below-cloud scavenging. Besides, considering the large amounts of particles (60-90
421 $\mu\text{g}/\text{m}^3$ in mass concentration) below-cloud in Beijing, the gases compounds may be not
422 as important as that in simulation in Japan. According to the yearly book of
423 “*Environmental Bulletin in Beijing*” from 1994 to 2017, the yearly concentration of SO_2
424 has a dramatically decreasing from 26.5 $\mu\text{g}/\text{m}^3$ in 2013 to 8 $\mu\text{g}/\text{m}^3$ in 2017. This
425 relatively low-level concentration of SO_2 at surface may not contribute a dominant role
426 in wet deposition of SO_4^{2-} . Similar case in NO_3^- , the ratio of gas-phase HNO_3 and the
427 total NO_3^- in the summer in Beijing is only 0.12 according to the measurement study of
428 Yue *et al.* (2013). The fraction of total inorganic nitrate as particulate nitrate instead of

429 gaseous nitric acid over the NCP increased from 90% in 2013 to 98% in 2017 (Zhai et
430 al., 2021), which means the gaseous nitric acid has been consumed by high level of
431 ammonia concentrations. We assumed the 10% ratio of gases added into the washout
432 process, which only leads to less 5% difference of below-cloud scavenging contribution
433 to total wet depositions. Anyway, for NH_3 , there might be larger uncertainties, since the
434 high concentration of NH_3 at ground surface over NCP (Pan et al., 2018). Kasper-Giebl
435 et al. (1999) reported that 49-79% of NH_4^+ in precipitation are from particulate
436 ammonium, which indicate the large uncertainties of contribution from gases still exists
437 in the form of NH_4^+ wet deposition. The uncertainties are mainly from the indistinct
438 window for the in-cloud scavenging judgement due to high concentration of gas NH_3
439 at ground surface which is not easy to be scavenged completely during the short time
440 fraction measurements. This is also confirmed by the larger difference in below-cloud
441 contribution to NH_4^+ wet deposition than other ions estimated by the exponential
442 approach and the average approach in Table 2. As it mentioned above, more longer
443 fraction measurements as well as the influence of NH_3 to NH_4^+ wet deposition are
444 needed in the future.

445 Following Eq (2), the contribution of below-cloud scavenging to wet deposition in
446 each rainfall event during 2014-2017 are estimated from the in-cloud concentration.
447 Figure 5 shows the yearly VWA of SNA and Ca^{2+} and the in-cloud and below-cloud
448 contributions. The ratio of below-cloud contribution to the four major components
449 based on the yearly median value of the in-cloud concentration is also shown in Figure
450 5. Benefiting from the Action Plan, the air quality at the surface layer have been
451 significantly improved (Zhang et al., 2019), which in turn leading to the decreases of
452 the below-cloud scavenging. In this study, it also shows the below-cloud contributions
453 of SO_4^{2-} , NO_3^- , NH_4^+ and Ca^{2+} decreases from >50% in 2014 to ~40% in 2017. In 2017,
454 the contribution of below-cloud scavenging declines to lower than 40% for SO_4^{2-} and
455 NH_4^+ , but remains at 44% for NO_3^- . Over the four-year period 2014-2017, the average
456 yearly wet deposition for all ions and the below-cloud wet scavenging contributions are
457 given in Table 2. Similar to the concentrations in precipitation, the wet deposition of
458 SO_4^{2-} , NO_3^- , NH_4^+ decreased from 21.5 $\text{kgS ha}^{-1} \text{ yr}^{-1}$, 8.9 and 19.0 $\text{kg N ha}^{-1} \text{ yr}^{-1}$ during

459 2007-2010 (Pan et al., 2012; 2013) to $11.4 \text{ kgS ha}^{-1} \text{ yr}^{-1}$ ($3.42 \times 10^3 \text{ mg m}^{-2} \text{ yr}^{-1}$), 6.9 and
460 $16.7 \text{ kgN ha}^{-1} \text{ yr}^{-1}$ (3.05×10^3 and $2.15 \times 10^3 \text{ mg m}^{-2} \text{ yr}^{-1}$) during 2014-2017, respectively.
461 Below-cloud scavenging contributed to almost half of total deposition estimated with
462 the exponential approach (50~60%), higher than the average approach (40~50%).

463 **4 Factors influencing below-cloud scavenging**

464 Each precipitation event is unique in terms rainfall intensity, droplet sizes and
465 distribution, rainfall type (thunderstorms or deep convective scavenging), air
466 concentrations of chemical components, etc. The unique characterization of each
467 precipitation event was considered in calculation of the proportions from in-cloud and
468 below-cloud processes, as the exponential approach to each unique event was made.
469 The below-cloud proportions varied from 20% to 80% among the 69 rainfall events.
470 The influence of these factors affecting wet scavenging were investigated through the
471 correlation analysis between below-cloud proportions with the rainfall type as well as
472 the rainfall intensity.

473 **4.1 Rainfall type**

474 The rainfall over the North China Plain in summer time is usually determined by the
475 synoptic system such as the upper-level trough or the cold vortex. The 69 rainfall events
476 have been classified based on synoptic system according to records from the Beijing
477 Meteorological Service (<http://bj.cma.gov.cn>) with 33 events associated with upper-
478 level troughs, 23 events associated with a cold vortex and 13 events associated with
479 other systems. Figure 6 shows the contributions of below-cloud scavenging for the two
480 major systems. A high contribution from below-cloud scavenging is found for rainfall
481 events associated with an upper-level trough with the median contributions for SO_4^{2-} ,
482 NO_3^- , NH_4^+ and Ca^{2+} of 56.2%, 62.1%, 56.3% and 61.9%, respectively. In the contrast,
483 the contributions during rainfall events under cold vortex conditions are significant
484 lower, with the values of 42.2%, 44.5%, 41.7% and 53.9%, respectively. Rainfall events
485 associated with an upper-level trough are usually accompanied by orographic or frontal
486 precipitation and are characterized by long and continuous precipitation (Shou et al.,
487 2000). This suggests that below-cloud scavenging of chemical components is important
488 for this rainfall type due to air mass transport from outside Beijing. In contrast, rainfall

489 events associated with a cold vortex usually originate from strong thermal convection
490 and are characterized by short heavy rainfall (Zhang et al., 2008;Liu et al., 2016;Zheng
491 et al., 2020). This is common during the summer months in Beijing with deep
492 convective clouds (Yu et al., 2011;Gao and He, 2013), and suggests that there is a large
493 contribution from in-cloud scavenging to the total wet deposition.

494 **4.2 Precipitation intensity and rainfall volume**

495 To illustrate the impacts of rainfall on below-cloud aerosol scavenging, the relationship
496 between the below-cloud fraction and the rainfall volume and precipitation intensity are
497 investigated, see Figure 7. Negative correlations in below cloud fraction are found for
498 both the rainfall volume and precipitation intensity, although the relationship with the
499 former is stronger (R: 0.63~0.93 vs. 0.03~0.64). This is consistent with results for 2014
500 in Beijing reported by Xu et al. (2017). Atmospheric particles are efficiently removed
501 below cloud by washout at the beginning of precipitation events (almost 70% of SNA
502 is removed in the first 2-3 fractions, as shown in Figure 1). As the rainfall progresses,
503 in-cloud scavenging makes an increasingly important contribution as below-cloud
504 aerosol concentrations fall. Xu et al. (2017) found that heavy summertime rainfall
505 events with more than 40 mm of rainfall usually occur over very short periods of time,
506 usually 2-3 h. This heavy rainfall leads to the scavenging of aerosols in a relatively
507 localized region and prevents the compensation associated with transport of air
508 pollutants from outside the region during longer-duration light rainfall events. This
509 contributes to the decreased contribution of below-cloud scavenging during the high
510 intensity rainfall events.

511 **5 Conclusions**

512 This paper presents an analysis of below-cloud scavenging from four years of
513 sequential sampling of rainfall events in Beijing from May of 2014 to November of
514 2017. The concentration of ions in precipitation varied dramatically, with yearly volume
515 weighted averaged concentrations of SO_4^{2-} , NO_3^- , NH_4^+ and Ca^{2+} decreasing by 39%,
516 12%, 25% and 35% between 2014 and 2017, respectively. Due to faster decreases in
517 SO_4^{2-} than NO_3^- both in precipitation and in the air during the observation period, there
518 is a significant decrease in S/N ratio in precipitation at 44% and in air at 48%.

519 Benefiting from the national Air Pollution Prevention and Control Action Plan, the
520 sulfur has been further reduced, while the nitrogen, especially nitrate, needs further
521 attention in the next Action Plan to prevent deterioration of the environment associated
522 with acid rain and photochemical pollution.

523 A new method has been developed and employed to estimate the below-cloud
524 contribution to wet deposition in Beijing. The new approach suggests that the
525 contribution from below-cloud scavenging is greater than that estimated applying
526 simpler approaches used in previous studies. Overall, the contribution of below-cloud
527 scavenging to the wet deposition of the four major components is important at 50~60%.
528 The contribution of below-cloud scavenging shows a decrease over the period 2014-
529 2017 for Ca^{2+} , SO_4^{2-} and NH_4^+ , but little change for NO_3^- during 2015-2017. Below-
530 cloud scavenging also has a strong cleansing effect on air pollution, and the hourly
531 concentration of $\text{PM}_{2.5}$ is found to decrease sharply as the rainfall events occur, even
532 with the effects from wind swept out have been accounted for.

533 Rainfall types also influence the contribution of below-cloud scavenging. Seventy-
534 five rainfall events during the four-year periods were classified based on the local
535 synoptic conditions. Lower contributions from below-cloud scavenging (~40%) are
536 found for the four major ions in rainfall events associated with a cold vortex, while
537 higher contributions (~60%) occurred associated with an upper-level trough.
538 Precipitation volume and intensity both show a negative correlation with the below-
539 cloud fraction. This suggests that atmospheric particles are efficiently removed via
540 below-cloud scavenging processes at the beginning of precipitation events. As the event
541 progresses, rainfall in the later fractions shows a greater contribution from in-cloud
542 scavenging processes as aerosols in the surface layer have already been removed. To
543 better understand the mechanism of below-cloud scavenging processes, high resolution
544 of measurement both in precipitation and in the air especially at the beginning of rainfall
545 events are needed in the future.

546

547 **Data availability.**

548 To request observed data for scientific research purposes, please contact Baozhu Ge at
549 the Institute of Atmospheric Physics, Chinese Academy of Sciences, via email
550 (gebz@mail.iap.ac.cn).

551

552 **Author contribution**

553 BG and ZW designed the whole structure of this work, and prepared the manuscript
554 with contributions from all co-authors. DX, XY, JW and QT helped with the data
555 processing. OW, XC and XP was involved in the scientific interpretation and discussion.

556

557 **Competing interests**

558 The authors declare that they have no conflict of interest

559

560 **Acknowledgment**

561 We appreciate CNEMC for providing the data of the 6 criteria pollutants in Beijing. We
562 also appreciate Beijing Municipal Environmental Monitoring Center for providing the
563 aerosol components data in Beijing. This work is supported by the National Natural
564 Science Foundation of China (Grant No 41877313, 91744206, 41620104008), Priority
565 Research Program (XDA19040204) and the Key Deployment Program (ZDRW-CN-
566 2018-1-03) of the Chinese Academy of Sciences.

567

568 **References:**

- 569 Aikawa, M., and Hiraki, T.: Washout/rainout contribution in wet deposition estimated
570 by 0.5 mm precipitation sampling/analysis, *Atmos Environ*, 43, 4935-4939, 2009.
- 571 Aikawa, M., Kajino, M., Hiraki, T., and Mukai, H.: The contribution of site to washout
572 and rainout: Precipitation chemistry based on sample analysis from 0.5 mm
573 precipitation increments and numerical simulation, *Atmos Environ*, 95, 165-174,
574 <http://dx.doi.org/10.1016/j.atmosenv.2014.06.015>, 2014.
- 575 Andronache, C.: Estimated variability of below-cloud aerosol removal by rainfall for
576 observed aerosol size distributions, *Atmospheric Chemistry and Physics*, 3, 131-
577 143, 2003.
- 578 Andronache, C.: Estimates of sulfate aerosol wet scavenging coefficient for locations
579 in the Eastern United States, *Atmospheric Environment*, 38, 795-804,
580 [10.1016/j.atmosenv.2003.10.035](http://dx.doi.org/10.1016/j.atmosenv.2003.10.035), 2004a.
- 581 Andronache, C.: Precipitation removal of ultrafine aerosol particles from the
582 atmospheric boundary layer, *J Geophys Res-Atmos*, 109, 2004b.
- 583 Bae, S. Y., Jung, C. H., and Kim, Y. P.: Derivation and verification of an aerosol
584 dynamics expression for the below-cloud scavenging process using the moment
585 method, *J Aerosol Sci*, 41, 266-280, 2010.
- 586 Bae, S. Y., Park, R. J., Yong, P. K., and Woo, J. H.: Effects of below-cloud scavenging
587 on the regional aerosol budget in East Asia, *Atmos Environ*, 58, p.14-22, 2012.
- 588 Barth, M. C., Rasch, P. J., Kiehl, J. T., Benkovitz, C. M., and Schwartz, S. E.: Sulfur
589 chemistry in the National Center for Atmospheric Research Community Climate
590 Model: Description, evaluation, features, and sensitivity to aqueous chemistry, *J*
591 *Geophys Res-Atmos*, 105, 1387-1415, 2000.
- 592 Bertrand, G., Celle-Jeanton, H., Laj, P., Rangognio, J., and Chazot, G.: Rainfall
593 chemistry: long range transport versus below cloud scavenging. A two-year study
594 at an inland station (Opme, France), *J Atmos Chem*, 60, 253-271, 2008.
- 595 Chate, D. M., Rao, P. S. P., Naik, M. S., Momin, G. A., Safai, P. D., and Ali, K.:
596 Scavenging of aerosols and their chemical species by rain, *Atmospheric*
597 *Environment*, 37, 2477-2484, [10.1016/S1352-2310\(03\)00162-6](http://dx.doi.org/10.1016/S1352-2310(03)00162-6), 2003.
- 598 Chen, L., Gao, Y., Zhang, M., Fu, J. S., Zhu, J., Liao, H., Li, J., Huang, K., Ge, B.,
599 Wang, X., Lam, Y. F., Lin, C. Y., Itahashi, S., Nagashima, T., Kajino, M., Yamaji,
600 K., Wang, Z., and Kurokawa, J.: MICS-Asia III: multi-model comparison and
601 evaluation of aerosol over East Asia, *Atmos. Chem. Phys.*, 19, 11911-11937,
602 Feng, J.: A size - resolved model for below - cloud scavenging of aerosols by snowfall,
603 *Journal of Geophysical Research*, 114, [10.1029/2008jd011012](http://dx.doi.org/10.1029/2008jd011012), 2009.
- 604 Gao, Y., and He, L. F.: The phase features of a cold vortex over north China (in English
605 abstract), *J Appl Meteor Sci*, 24, 704-713, 2013.
- 606 Ge, B., Wang, Z., Gbaguidi, A. E., and Zhang, Q.: Source Identification of Acid Rain
607 Arising over Northeast China: Observed Evidence and Model Simulation, *Aerosol*
608 *Air Qual Res*, 16, 1366-1377, [10.4209/aaqr.2015.05.0294](http://dx.doi.org/10.4209/aaqr.2015.05.0294), 2016.
- 609 Ge, B., Itahashi, S., Sato, K., Xu, D., Wang, J., Fan, F., Tan, Q., Fu, J. S., Wang, X.,
610 Yamaji, K., Nagashima, T., Li, J., Kajino, M., Liao, H., Zhang, M., Wang, Z., Li,

611 M., Woo, J. H., Kurokawa, J., Pan, Y., Wu, Q., Liu, X., and Wang, Z.: MICS-Asia
612 III: Multi-model comparison of reactive Nitrogen deposition over China, *Atmos.*
613 *Chem. Phys. Discuss.*, 2020, 1-43, 10.5194/acp-2019-1083, 2020.

614 Goncalves, F. L. T., Ramos, A. M., Freitas, S., Dias, M. A. S., and Massambani, O.: In-
615 cloud and below-cloud numerical simulation of scavenging processes at Serra Do
616 Mar region, SE Brazil, *Atmos Environ*, 36, 5245-5255, 2002.

617 Gryspeerdt, E., Stier, P., White, B. A., and Kipling, Z.: Wet scavenging limits the
618 detection of aerosol effects on precipitation, *Atmos. Chem. Phys.*, 15, 7557-7570,
619 10.5194/acp-15-7557-2015, 2015.

620 Henzing, J. S., Olivie, D. J. L., and van Velthoven, P. F. J.: A parameterization of size
621 resolved below cloud scavenging of aerosols by rain, *Atmospheric Chemistry and*
622 *Physics*, 6, 3363-3375, 2006.

623 Hicks, B. B.: A climatology of wet deposition scavenging ratios for the United States,
624 *Atmos Environ*, 39, 1585-1596, 2005.

625 Huang, M., Shen, Z., and Liu, S.: A study on the formation processes of acid rain in
626 some areas of Southwest China (in Chinese), *Scientia Atmospherica Sinica*, 19, 359-
627 366, 1995.

628 Itahashi, S., Yumimoto, K., Uno, I., Hayami, H., Fujita, S. I., Pan, Y., and Wang, Y.: A
629 15-year record (2001–2015) of the ratio of nitrate to non-sea-salt sulfate in
630 precipitation over East Asia, *Atmos. Chem. Phys.*, 18, 2835-2852, 10.5194/acp-18-
631 2835-2018, 2018.

632 Itahashi, S., Ge, B., Sato, K., Fu, J. S., Wang, X., Yamaji, K., Nagashima, T., Li, J.,
633 Kajino, M., Liao, H., Zhang, M., Wang, Z., Li, M., Kurokawa, J., Carmichael, G.
634 R., and Wang, Z.: MICS-Asia III: overview of model intercomparison and
635 evaluation of acid deposition over Asia, *Atmos. Chem. Phys.*, 20, 2667-2693,
636 10.5194/acp-20-2667-2020, 2020.

637 Kasper-Giebl, A., Kalina, M. F., and Puxbaum, H.: Scavenging ratios for sulfate,
638 ammonium and nitrate determined at Mt. Sonnblick (3106 m asl), *Atmos Environ*,
639 33, 895-906, 1999.

640 Kong, L., Tang, X., Zhu, J., Wang, Z., Fu, J. S., Wang, X., Itahashi, S., Yamaji, K.,
641 Nagashima, T., Lee, H. J., Kim, C. H., Lin, C. Y., Chen, L., Zhang, M., Tao, Z., Li,
642 J., Kajino, M., Liao, H., Wang, Z., Sudo, K., Wang, Y., Pan, Y., Tang, G., Li, M.,
643 Wu, Q., Ge, B., and Carmichael, G. R.: Evaluation and uncertainty investigation of
644 the NO₂, CO and NH₃ modeling over China under the framework of MICS-
645 Asia III, *Atmos. Chem. Phys.*, 20, 181-202, 10.5194/acp-20-181-2020, 2020.

646 Li, R., Cui, L., Zhao, Y., Zhang, Z., Sun, T., Li, J., Zhou, W., Meng, Y., Huang, K., and
647 Fu, H.: Wet deposition of inorganic ions in 320 cities across China: spatio-temporal
648 variation, source apportionment, and dominant factors, *Atmos. Chem. Phys.*, 19,
649 11043-11070, 10.5194/acp-19-11043-2019, 2019.

650 Liu, X. M., Zhang, M. J., Wang, S. J., Zhao, P. P., Wang, J., and Zhou, P. P.: Estimation
651 and analysis of precipitation cloud base height in China (in english abstract),
652 *Meteor Mon*, 42, 1135-1145, 2016.

653 Malaguti, A., Mircea, M., La Torretta, T. M. G., Telloli, C., Petralia, E., Stracquadiano,
654 M., and Berico, M.: Comparison of Online and Offline Methods for Measuring

655 Fine Secondary Inorganic Ions and Carbonaceous Aerosols in the Central
656 Mediterranean Area, *Aerosol Air Qual Res*, 15, 2641-2653, 2015.

657 Markovic, M. Z., VandenBoer, T. C., and Murphy, J. G.: Characterization and
658 optimization of an online system for the simultaneous measurement of atmospheric
659 water-soluble constituents in the gas and particle phases, *J Environ Monitor*, 14,
660 1872-1884, 2012.

661 Okita, T., Hara, H., and Fukuzaki, N.: Measurements of atmospheric SO₂ and SO₄²⁻,
662 and determination of the wet scavenging coefficient of sulfate aerosols for the
663 winter monsoon season over the Sea of Japan, *Atmos Environ*, 30, 3733-3739,
664 1996.

665 Ouyang, W., Guo, B. B., Cai, G. Q., Li, Q., Han, S., Liu, B., and Liu, X. G.: The washing
666 effect of precipitation on particulate matter and the pollution dynamics of rainwater
667 in downtown Beijing, *Sci Total Environ*, 505, 306-314, 2015.

668 Pan, Y. P., Wang, Y. S., Tang, G. Q., and Wu, D.: Wet and dry deposition of atmospheric
669 nitrogen at ten sites in Northern China, *Atmos Chem Phys*, 12, 6515-6535, 2012.

670 Pan, Y. P., Wang, Y. S., Tang, G. Q., and Wu, D.: Spatial distribution and temporal
671 variations of atmospheric sulfur deposition in Northern China: insights into the
672 potential acidification risks, *Atmos Chem Phys*, 13, 1675-1688, 2013.

673 Pan, Y. P., Tian, S. L., Zhao, Y. H., Zhang, L., Zhu, X. Y., Gao, J., Huang, W., Zhou, Y.
674 B., Song, Y., Zhang, Q., and Wang, Y. S.: Identifying Ammonia Hotspots in China
675 Using a National Observation Network, *Environ Sci Technol*, 52, 3926-3934,
676 10.1021/acs.est.7b05235, 2018.

677 Pu, W. W., Quan, W. J., Ma, Z. L., Shi, X. F., Zhao, X. J., Zhang, L. N., Wang, Z. F.,
678 and Wang, W. Y.: Long-term trend of chemical composition of atmospheric
679 precipitation at a regional background station in Northern China, *Sci Total Environ*,
680 580, 1340-1350, 2017.

681 Seinfeld, J. H., and Pandis, S. N.: *Atmospheric chemistry and physics: from air
682 pollution to climate change*, Wiley, New York, 2006.

683 Shou, S. W., Zhu, Q. G., Lin, J. R., and Tang, D. S.: *The principles and methods of
684 weather science[M]*, China Meteorological Press, Beijing, 76-81 pp., 2000.

685 Sportisse, B.: A review of parameterizations for modelling dry deposition and
686 scavenging of radionuclides, *Atmospheric Environment*, 41, 2683-2698,
687 10.1016/j.atmosenv.2006.11.057, 2007.

688 State Council of the People's Republic of China, Notice of the general office of the state
689 council on issuing the air pollution prevention and control action plan.
690 http://www.gov.cn/zwggk/2013-09/12/content_2486773.htm. Accessed 21 August
691 2019.

692 Sun, Y. L., Wang, Z. F., Du, W., Zhang, Q., Wang, Q. Q., Fu, P. Q., Pan, X. L., Li, J.,
693 Jayne, J., and Worsnop, D. R.: Long-term real-time measurements of aerosol
694 particle composition in Beijing, China: seasonal variations, meteorological effects,
695 and source analysis, *Atmos Chem Phys*, 15, 10149-10165, 2015.

696 Tan, J., Fu, J. S., Carmichael, G. R., Itahashi, S., Tao, Z., Huang, K., Dong, X., Yamaji,
697 K., Nagashima, T., Wang, X., Liu, Y., Lee, H. J., Lin, C. Y., Ge, B., Kajino, M.,
698 Zhu, J., Zhang, M., Liao, H., and Wang, Z.: Why do models perform differently on

699 particulate matter over East Asia? A multi-model intercomparison study for MICS-
700 Asia III, *Atmos. Chem. Phys.*, 20, 7393-7410, 10.5194/acp-20-7393-2020, 2020.

701 Tang, A. H., Zhuang, G. S., Wang, Y., Yuan, H., and Sun, Y. L.: The chemistry of
702 precipitation and its relation to aerosol in Beijing, *Atmos Environ*, 39, 3397-3406,
703 DOI 10.1016/j.atmosenv.2005.02.001, 2005.

704 Tang, J. C. H. B., Yu, X. L., Wang, S., Yao, P., Lv, B., Xu, X. B., and Ding, G.:
705 Evaluation of results of station inter-comparison with blind samples in Acid Rain
706 Monitoring Network in China, *Meteoro. Monthly*, 33, 75–83, 2007 (in English
707 abstract).

708 Tang, J., Xu, X., Ba, J., and Wang, S.: Trends of the precipitation acidity over China
709 during 1992–2006, *Chinese. Sci. Bul.*, 5, 1800–1807, doi:10.1007/s11434-009-
710 3618-1, 2010.

711 Textor, C., Schulz, M., Guibert, S., Kinne, S., Balkanski, Y., Bauer, S., Berntsen, T.,
712 Berglen, T., Boucher, O., Chin, M., Dentener, F., Diehl, T., Easter, R., Feichter, H.,
713 Fillmore, D., Ghan, S., Ginoux, P., Gong, S., Kristjansson, J. E., Krol, M., Lauer,
714 A., Lamarque, J. F., Liu, X., Montanaro, V., Myhre, G., Penner, J., Pitari, G., Reddy,
715 S., Seland, O., Stier, P., Takemura, T., and Tie, X.: Analysis and quantification of
716 the diversities of aerosol life cycles within AeroCom, *Atmos Chem Phys*, 6, 1777-
717 1813, 2006.

718 Tian, S. L., Pan, Y. P., and Wang, Y. S.: Size-resolved source apportionment of
719 particulate matter in urban Beijing during haze and non-haze episodes, *Atmos
720 Chem Phys*, 16, 1-19, 10.5194/acp-16-1-2016, 2016.

721 Vet, R., Artz, R. S., Carou, S., Shaw, M., Ro, C. U., Aas, W., Baker, A., Bowersox, V.
722 C., Dentener, F., Galy-Lacaux, C., Hou, A., Pienaar, J. J., Gillett, R., Forti, M. C.,
723 Gromov, S., Hara, H., Khodzher, T., Mahowald, N. M., Nickovic, S., Rao, P. S. P.,
724 and Reid, N. W.: A global assessment of precipitation chemistry and deposition of
725 sulfur, nitrogen, sea salt, base cations, organic acids, acidity and pH, and
726 phosphorus, *Atmos Environ*, 93, 3-100, 2014.

727 Wang, W. X., and Wang, T.: On acid rain formation in China, *Atmos Environ*, 30, 4091-
728 4093, 1996.

729 Wang, X., Zhang, L., and Moran, M. D.: Uncertainty assessment of current size-
730 resolved parameterizations for below-cloud particle scavenging by rain, *Atmos.
731 Chem. Phys.*, 10, 5685-5705, 10.5194/acp-10-5685-2010, 2010.

732 Wang, X., Zhang, L., and Moran, M. D.: Development of a new semi-empirical
733 parameterization for below-cloud scavenging of size-resolved aerosol particles by
734 both rain and snow, *Geosci Model Dev*, 7, 799-819, 10.5194/gmd-7-799-2014,
735 2014.

736 Wang, Y., Xue, L. I., Li, Y. A. O., Yanan, Z., and Yuepeng, P. A. N.: Variation of pH and
737 Chemical Composition of Precipitation by Multi-step Sampling in Summer of
738 Beijing 2007 (in english abstract), 30, 2715-2721, 2009.

739 Wang, Z. F., Xie, F. Y., Sakurai, T., Ueda, H., Han, Z. W., Carmichael, G. R., Streets,
740 D., Engardt, M., Holloway, T., Hayami, H., Kajino, M., Thongboonchoo, N.,
741 Bennet, C., Park, S. U., Fung, C., Chang, A., Sartelet, K., and Amann, M.: MICS-
742 Asia II: Model inter-comparison and evaluation of acid deposition, *Atmos Environ*,

743 42, 3528-3542, 2008.

744 Xu, D., Ge, B., Chen, X., Sun, Y., Cheng, N., Li, M., Pan, X., Ma, Z., Pan, Y., and Wang,
745 Z.: Multi-method determination of the below-cloud wet scavenging coefficients of
746 aerosols in Beijing, China, *Atmos. Chem. Phys.*, 19, 15569-15581, 10.5194/acp-
747 19-15569-2019, 2019.

748 Xu, D. H., Ge, B. Z., Wang, Z. F., Sun, Y. L., Chen, Y., Ji, D. S., Yang, T., Ma, Z. Q.,
749 Cheng, N. L., Hao, J. Q., and Yao, X. F.: Below-cloud wet scavenging of soluble
750 inorganic ions by rain in Beijing during the summer of 2014, *Environ Pollut*, 230,
751 963-973, 10.1016/j.envpol.2017.07.033, 2017.

752 Yamagata, S., Kobayashi, D., Ohta, S., Murao, N., Shiobara, M., Wada, M., Yabuki, M.,
753 Konishi, H., and Yamanouchi, T.: Properties of aerosols and their wet deposition in
754 the arctic spring during ASTAR2004 at Ny-Alesund, Svalbard, *Atmos Chem Phys*,
755 9, 261-270, 2009.

756 Yang, F., Tan, J., Shi, Z. B., Cai, Y., He, K., Ma, Y., Duan, F., Okuda, T., Tanaka, S., and
757 Chen, G.: Five-year record of atmospheric precipitation chemistry in urban Beijing,
758 China, *Atmos Chem Phys*, 12, 2025-2035, DOI 10.5194/acp-12-2025-2012, 2012.

759 Yu, Z. Y., He, L. F., Fan, G. Z., Li, Z. C., and Su, Y. L.: The basic features of the severe
760 convection at the background of cold vortex over north china (in English abstract),
761 *J Trop Meteor*, 27, 89-94, 2011.

762 Yuan, W. H., Sun, W., Chen, H. M., and Yu, R. C.: Topographic effects on
763 spatiotemporal variations of short-duration rainfall events in warm season of
764 central North China, *J Geophys Res-Atmos*, 119, 11223-11234, 2014.

765 Zhai S., D. J. Jacob, X. Wang, Z. Liu, T. Wen, V. Shah, K. Li, J. Moch, K. H. Bates, S.
766 Song, L. Shen, Y. Zhang, G. Luo, F. Yu, Y. Sun, L. Wang, M. Qi, J. Tao, K. Gui, H.
767 Xu, Q. Zhang, T. Zhao, H. C. Lee, H. Choi, H. Liao, Control of particulate nitrate
768 air pollution in China, *Nature Geoscience*, in press, 2021

769 Zhang, C., Zhang, Q., Wang, Y., and Liang, X.: Climatology of warm season cold
770 vortices in East Asia: 1979-2005, *Meteorol Atmos Phys*, 100, 291-301, 2008.

771 Zhang, L., Michelangeli, D. V., and Taylor, P. A.: Numerical studies of aerosol
772 scavenging by low-level, warm stratiform clouds and precipitation, *Atmos Environ*,
773 38, 4653-4665, <https://doi.org/10.1016/j.atmosenv.2004.05.042>, 2004.

774 Zhang, L., Wang, X., Moran, M. D., and Feng, J.: Review and uncertainty assessment
775 of size-resolved scavenging coefficient formulations for below-cloud snow
776 scavenging of atmospheric aerosols, *Atmospheric Chemistry and Physics*, 13,
777 10005-10025, 10.5194/acp-13-10005-2013, 2013.

778 Zhang, Q., Zheng, Y. X., Tong, D., Shao, M., Wang, S. X., Zhang, Y. H., Xu, X. D.,
779 Wang, J. N., He, H., Liu, W. Q., Ding, Y. H., Lei, Y., Li, J. H., Wang, Z. F., Zhang,
780 X. Y., Wang, Y. S., Cheng, J., Liu, Y., Shi, Q. R., Yan, L., Geng, G. N., Hong, C. P.,
781 Li, M., Liu, F., Zheng, B., Cao, J. J., Ding, A. J., Gao, J., Fu, Q. Y., Huo, J. T., Liu,
782 B. X., Liu, Z. R., Yang, F. M., He, K. B., and Hao, J. M.: Drivers of improved
783 PM_{2.5} air quality in China from 2013 to 2017, *P Natl Acad Sci USA*, 116, 24463-
784 24469, 2019.

785 Zheng, B., Tong, D., Li, M., Liu, F., Hong, C., Geng, G., Li, H., Li, X., Peng, L., Qi, J.,
786 Yan, L., Zhang, Y., Zhao, H., Zheng, Y., He, K., and Zhang, Q.: Trends in China's

787 anthropogenic emissions since 2010 as the consequence of clean air actions, Atmos.
788 Chem. Phys. Discuss., 2018, 1-27, 10.5194/acp-2018-374, 2018.
789 Zheng, Y. F., Wang L. W., and Du, J. Y.: Comparative Analysis of the Features of
790 Precipitating and Nonprecipitating Ice Clouds in the BeijingTianjin-Hebei Region
791 in Summer (in english abstract), Climatic and Environmental Research, 25, 77-89,
792 10.3878/j.issn.1006-9585.2019.18091, 2020.
793

794

795 Table 1. Correlation of the concentrations of major ions in air in the six hours before
796 rainfall with those in precipitation. Pearson correlation coefficients are presented for
797 monthly volume weighted average (VWA) concentrations and for the first fraction (F1[#])
798 in each event.

	SO₄²⁻ (n=13)	NO₃⁻ (n=14)	NH₄⁺ (n=13)	Ca²⁺ (n=9)
VWA	0.70 ^a	0.53 ^b	0.65 ^a	0.47
F1 [#]	0.76 ^a	0.62 ^a	0.77 ^a	0.85 ^a

799 Note: "a" and "b" represent significant correlations at $p < 0.01$ and $p < 0.05$, respectively.

800

801

802 Table 2. Exponential fitting for the concentrations of major ions in different fractions of rainfall, and the contribution of below-cloud scavenging
 803 to total deposition.

Chemical component	Exponential Fitting for 50 th percentile ^a	R ² (n=11)	Asymptote value (mg/L)	Below cloud % ^b	Average of F6#-F8# (mg/L)	Below cloud % ^c	Difference % ^d	Total wet deposition (mg/m ² /yr)
SO ₄ ²⁻	y=3.17+10.28 e ^{-0.51x}	0.85	3.18	50%	3.33	48%	<3%	3423.3
NO ₃ ⁻	y=2.32+11.03 e ^{-0.45x}	0.81	2.32	59%	2.59	54%	<6%	3046.5
NH ₄ ⁺	y=1.39+5.81 e ^{-0.28x}	0.79	1.39	65%	1.95	51%	<9%	2149.5
Ca ²⁺	y=0.67+6.81 e ^{-0.6x}	0.93	0.67	52%	0.72	48%	<6%	746.0
F ⁻	y=0.04+0.24 e ^{-0.34x}	0.91	0.04	56%	0.05	40%	<10%	49.0
Cl ⁻	y=0.27+2.2 e ^{-0.6x}	0.95	0.27	53%	0.29	50%	<5%	309.7
Na ⁺	y=0.1+1.34 e ^{-0.94x}	0.91	0.10	64%	0.10	64%	<1%	150.6
K ⁺	y=0.06+0.49 e ^{-0.47x}	0.89	0.06	64%	0.07	58%	<9%	89.8
Mg ²⁺	y=0.08+0.81 e ^{-0.4x}	0.83	0.08	61%	0.11	46%	<13%	109.2

804 ^a fitting for the median of each fraction in different rainfall events; ^b below cloud portion calculated based on the fitting curve; ^c below cloud portion
 805 calculated based on the average value of fractions 6 to 8 (F6#~F8#) in rainfall events; ^d difference in concentrations between adjacent 1 mm
 806 increments after 5 mm accumulated precipitation.

809 **Figures and captions**

810 **Figure 1.** Concentrations of SO_4^{2-} (a), NO_3^- (b), NH_4^+ (c) and Ca^{2+} (d) in each 1-mm
811 fraction of rainfall (i.e., F1#, F2#, ...) over different rainfall events in the observation
812 periods. The red line shows an exponential fitting using the 50th percentile of the data
813 and the red shading indicates the range between the 25th and 75th percentiles.

814 **Figure 2.** Time series of annual volume weighted average (VWA) concentration and
815 wet deposition of the four major components NH_4^+ (a), Ca^{2+} (b), SO_4^{2-} (c) and NO_3^- (d)
816 in precipitation in Beijing.

817 **Figure 3.** Annual changes in emission and concentration of SO_2 and NO_x in Beijing,
818 data is collected from the yearly book of “*Environmental Bulletin in Beijing*” from 1994
819 to 2017.

820 **Figure 4.** Relationships between the concentration of NO_3^- (a), SO_4^{2-} (b), NH_4^+ (c) and
821 Ca^{2+} (d) in precipitation and in air in the 6 h before each precipitation event. The red
822 square and blue triangle represented the relationships between the concentration of ions
823 in air with that in F1# and in VWA, respectively.

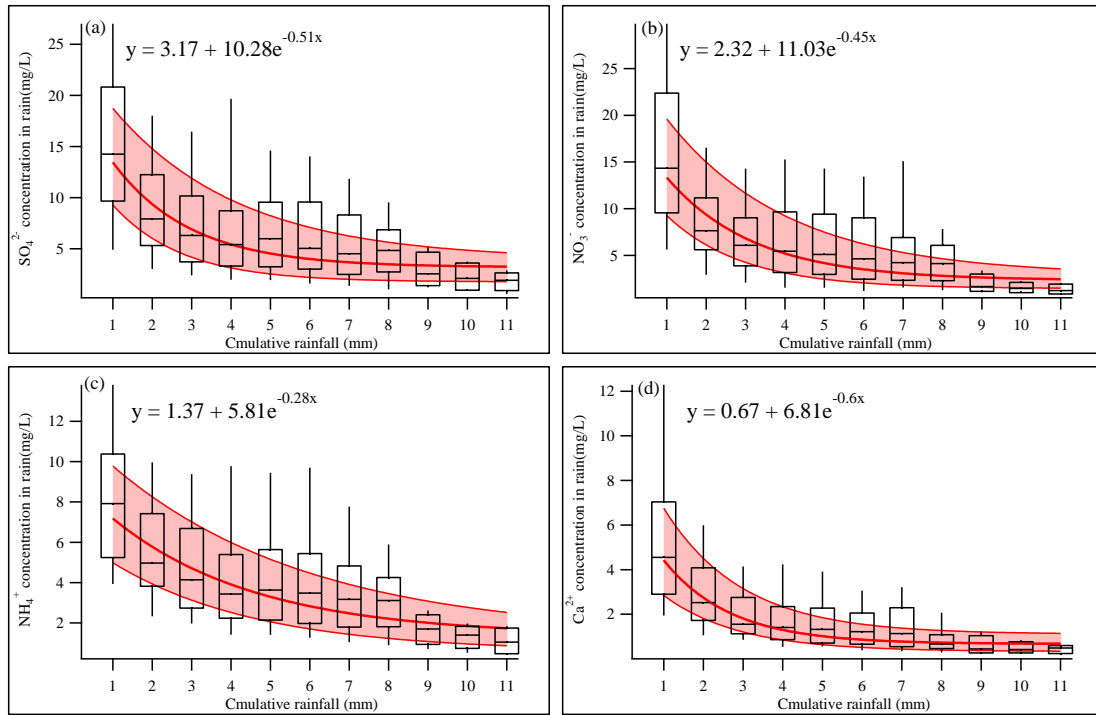
824 **Figure 5.** The annual volume weighted average below-cloud and in-cloud portion of
825 SO_4^{2-} (a), Ca^{2+} (b), NO_3^- (c), and NH_4^+ (d) during 2014-2017. The ratio of annual
826 median below-cloud contribution for each component is represented as the black line
827 in each panel. The mark #M and #A in the ratio of below-cloud represent the estimation
828 based on the median value and average value of in-cloud concentration in each year,
829 while the first quartile and the third quartiles are also included in the figure.

830 **Figure 6.** Contribution of below-cloud scavenging during rainfall events associated
831 with different synoptic conditions.

832 **Figure 7.** Contribution of below-cloud scavenging in events with different rainfall
833 volume and precipitation intensity

834

835



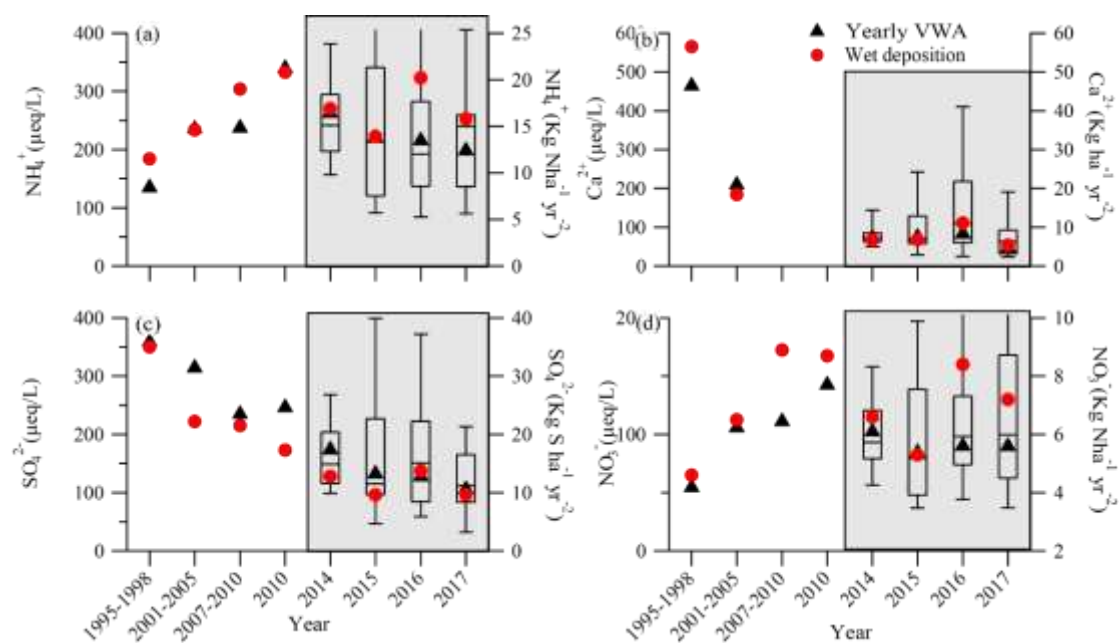
837

838 Figure 1. Concentrations of SO_4^{2-} (a), NO_3^- (b), NH_4^+ (c) and Ca^{2+} (d) in each 1-mm
 839 fraction of rainfall (i.e., F1#, F2#, ...) over different rainfall events in the observation
 840 periods. The red line shows an exponential fitting using the 50th percentile of the data
 841 and the red shading indicates the range between the 25th and 75th percentiles.

842

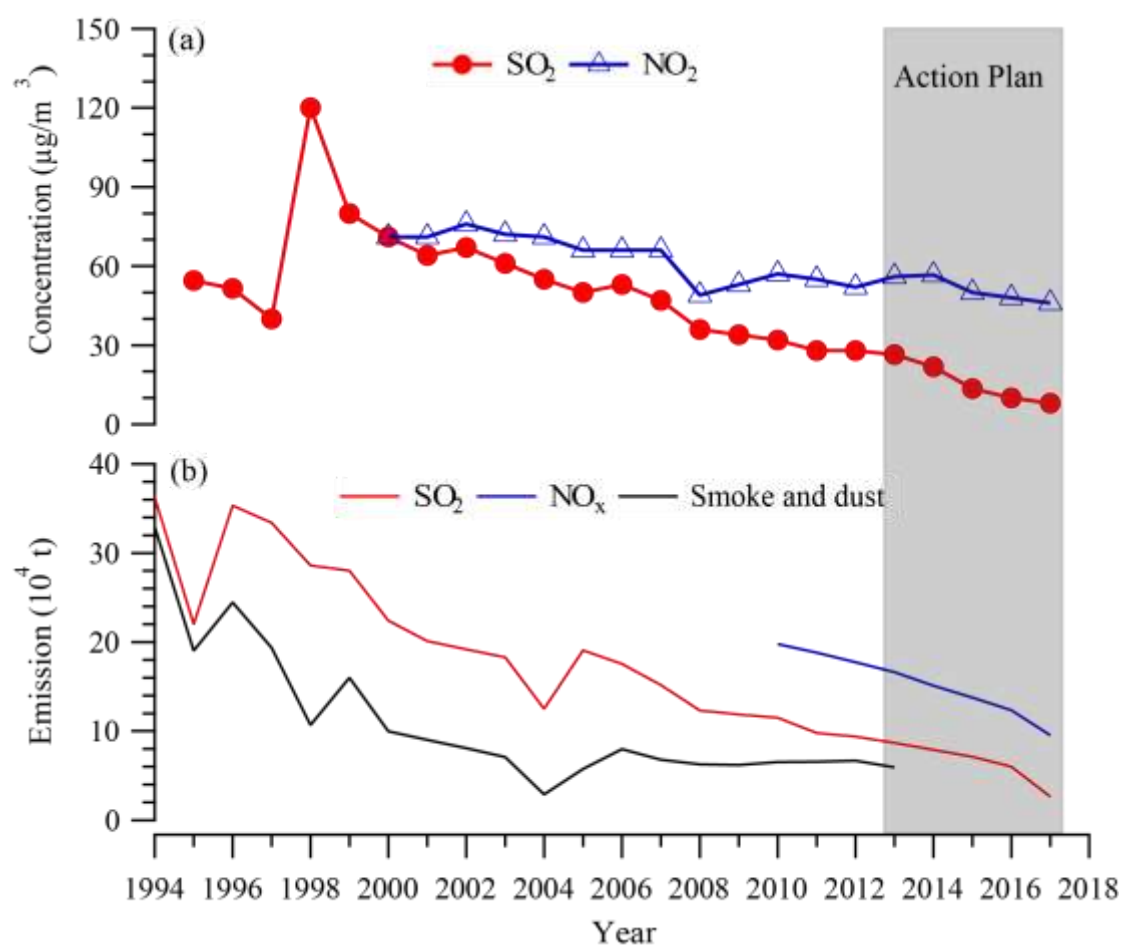
843

844



845

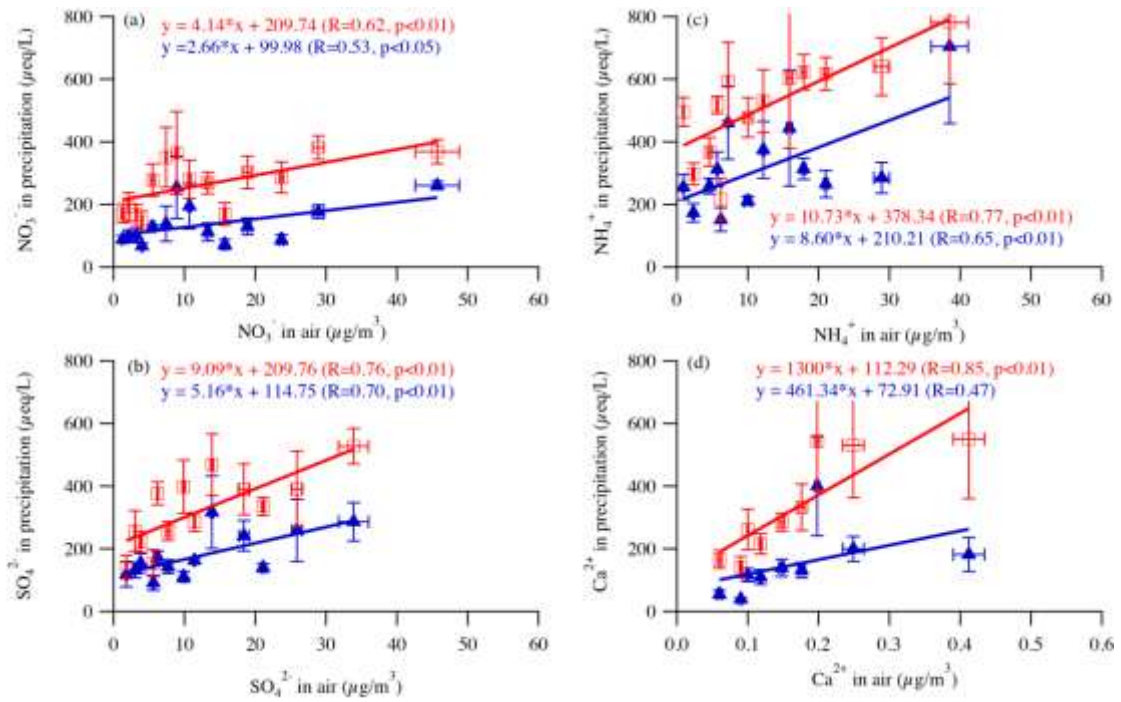
846 Figure 2. Time series of annual volume weighted average (VWA) concentration and
847 wet deposition of the four major components NH_4^+ (a), Ca^{2+} (b), SO_4^{2-} (c) and NO_3^-
848 (d) in precipitation in Beijing.



850

851 Figure 3. Annual changes in emission and concentration of SO₂ and NO_x in Beijing,
 852 data is collected from the yearly book of “*Environmental Bulletin in Beijing*” from
 853 1994 to 2017.

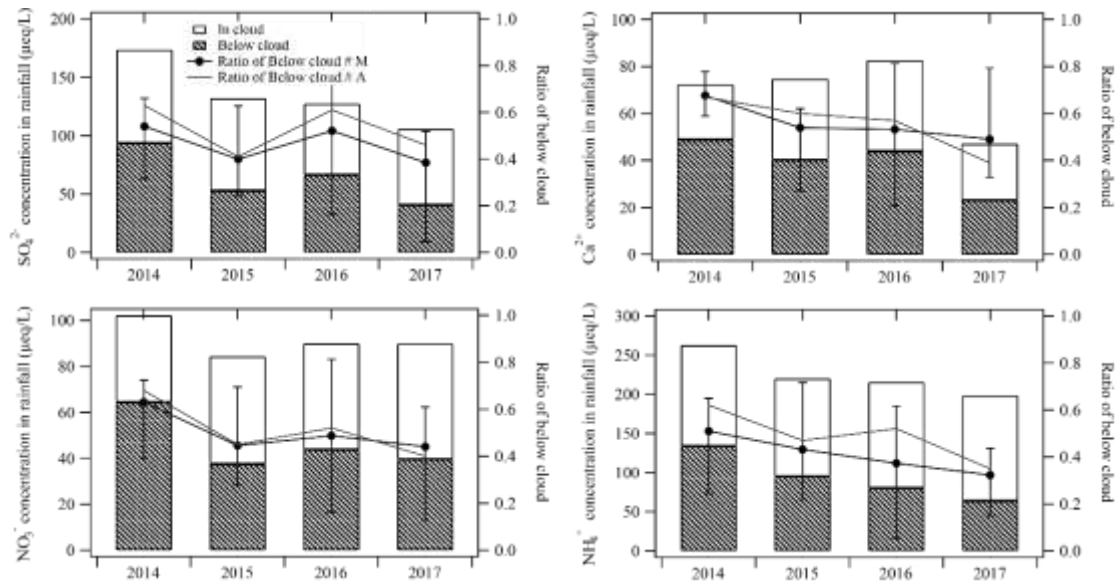
854



855

856 Figure 4. Relationships between the concentration of NO_3^- (a), SO_4^{2-} (b), NH_4^+ (c) and
857 Ca^{2+} (d) in precipitation and in air in the 6 h before each precipitation event. The red
858 square and blue triangle represented the relationships between the concentration of ions
859 in air with that in F1# and in VWA, respectively.

860

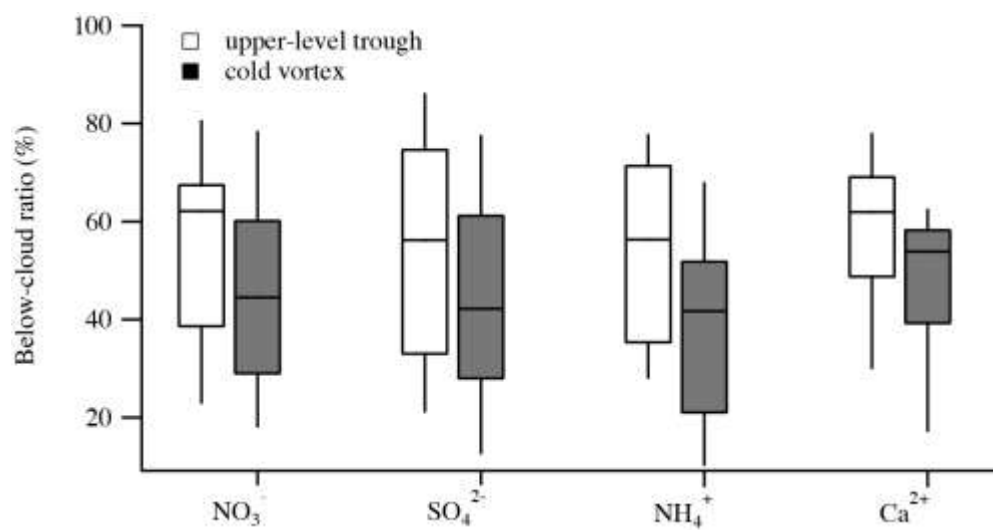


861

862 Figure 5. The annual volume weighted average below-cloud and in-cloud portion of
863 SO_4^{2-} (a), Ca^{2+} (b), NO_3^- (c), and NH_4^+ (d) during 2014-2017. The ratio of annual
864 median below-cloud contribution for each component is represented as the black line
865 in each panel. The mark #M and #A in the ratio of below-cloud represent the estimation
866 based on the median value and average value of in-cloud concentration in each year,
867 while the first quartile and the third quartiles are also included in the figure.

868

869

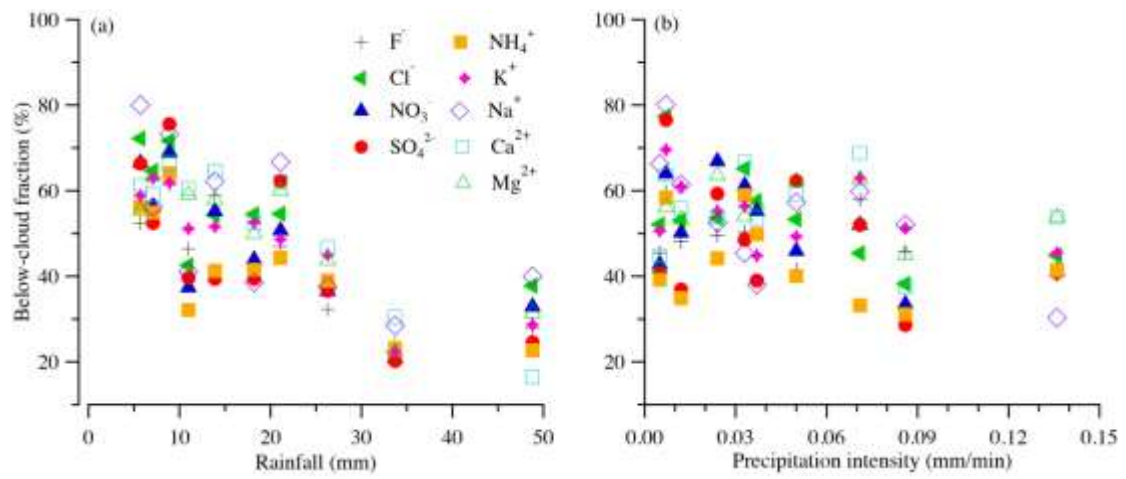


870

871 Figure 6. Contribution of below-cloud scavenging during rainfall events associated
872 with different synoptic conditions.

873

874



875

876 Figure 7. Contribution of below-cloud scavenging in events with different rainfall
877 volume and precipitation intensity.